

*Large Hadron Collider Project*

**LHC Project Report 251**

## **Strand Coating for the Superconducting Cables of the LHC Main Magnets**

D. Richter, J. D. Adam, D. Leroy, L. R. Oberli

### **Abstract**

The electrical resistance of contacts between strands in the Rutherford type superconducting cables has a major effect on the eddy current loss in cables, and on the dynamic magnetic field error in the LHC main magnets. In order to guarantee the value and constancy of the contact resistance, various metallic coatings were studied from the electrical and mechanical points of view in the past.

We report on the molten bath  $\text{Sn}_{95\text{wt.}}\text{Ag}_{5\text{wt.}}$  coating, oxidized thermally in air after the cabling is completed, that we adopted for the cables of the LHC main magnets. The value of the contact resistance is determined by the strand coating and cabling procedures, oxidation heat treatment, and the magnet coil cu-ring and handling. Chemical analysis helps to understand the evolution of the contacts.

We also mention results on two electrolytic coatings resulting in higher contact resistance.

CERN, LHC Division – Geneva, Switzerland

Presented at ASC'98 Superconductivity Conference, Palm Spring, CA, USA, September 1998

Administrative Secretariat  
LHC Division  
CERN  
CH - 1211 Geneva 23  
Switzerland

Geneva, 7 October 1998

# Strand Coating for the Superconducting Cables of the LHC Main Magnets

D. Richter, J. D. Adam, D. Leroy, L. R. Oberli  
CERN, CH-1211 Geneva 23, Switzerland

**Abstract**— The electrical resistance of contacts between strands in the Rutherford type superconducting cables has a major effect on the eddy current loss in cables, and on the dynamic magnetic field error in the LHC main magnets. In order to guarantee the value and constancy of the contact resistance, various metallic coatings were studied from the electrical and mechanical points of view in the past.

We report on the molten bath Sn<sub>95wt</sub>Ag<sub>5wt</sub> coating, oxidized thermally in air after the cabling is completed, that we adopted for the cables of the LHC main magnets. The value of the contact resistance is determined by the strand coating and cabling procedures, oxidation heat treatment, and the magnet coil curing and handling. Chemical analysis helps to understand the evolution of the contacts.

We also mention results on two electrolytic coatings resulting in higher contact resistance.

## I. INTRODUCTION

The coils of the LHC dipoles and quadrupoles [1] are made of two layers of 15.1 mm wide Rutherford type superconducting cable. The dipole coils have a different cable in each layer.

The cable for the inner dipole coil (Cable 1) is made of 28 strands 1.065 mm in diameter. The cable for the outer dipole coil and for both the inner and outer quadrupole coils (Cable 2) is made of 36 strands 0.825 mm in diameter. The LHC main dipoles and quadrupoles will require the fabrication of around 6900 km of superconducting cable.

In the Rutherford type cable strands touch in 3 types of contacts: strands from opposite faces of the cable form crossing contacts with electrical resistance  $R_c$ , neighboring strands form (on most of their length) adjacent contacts with resistance  $R_A$ , while on the cable edges they form more complex contacts related to  $R_A$  and  $R_c$ . We define  $R_c$  as the resistance per one cross-over of two strands. We define  $R_A$  as the resistance between two adjacent strands normalized per crossing contact.

As manufactured, the cable has a contact resistance  $R_{C,Mnf}$ . A coil is wound from that cable, and cured in a press at 190 °C for 0.5 h (standard curing) in order to obtain its precise form, and to glue the polyimide insulation of the cable. Due to the curing the contact resistance drops to a new value  $R_{C,Crd}$ . Before the coil is mounted in a magnet, the inter-strand contacts may reopen. This increases the contact resistance to  $R_{C,Rlx} \cong R_{C,Mnf}$ . Therefore in a magnet the resistance  $R_{C,Mgn}$  is  $R_{C,Crd} \leq R_{C,Mgn} \leq R_{C,Rlx}$ .

During the excitation of the magnets, coupling currents are induced between the strands of the cable, resulting in dynamic distortions of the magnetic field, and in energy losses.

These effects are proportional to dB/dt and inversely proportional to  $R_c$ . The inner layer of the LHC dipoles is the main source of field error and Joule heating.

The value of  $R_c$ , suitable for the main LHC magnets, is limited at its minimum by constraints on the dynamic magnetic field error and the energy losses. At its maximum,  $R_c$  is limited by the cable stability against thermal excitation [2], and uneven current distribution between strands due to non-uniform cable-to-cable  $R_c$ , and boundary-induced coupling currents [3]. Based on a theoretical study [4] and the measurement of dynamic field errors, the Cable 1  $R_{C,Mgn}$  should be  $\geq 15 \mu\Omega$ , and the Cable 2  $R_{C,Mgn} \geq 30 \mu\Omega$  [5]. The R&D work aims at 20 and 40  $\mu\Omega$  respectively.

The effect of  $R_A$  on the magnetic field errors is not significant as long as  $R_A \geq 0.2 \mu\Omega$  [6]. We will not discuss  $R_A$  as  $R_A \gg 0.2 \mu\Omega$  in all cables mentioned in this paper.

In order to guarantee the specified  $R_{C,Mgn}$  in the superconducting cables for the LHC, an R&D program, described in [7], was started at CERN. Within the program we studied properties of different coatings. We selected the molten bath deposited Sn<sub>95wt</sub>Ag<sub>5wt</sub>, electrolytic Cu<sub>55wt</sub>Sn<sub>45wt</sub> and Sn<sub>65wt</sub>Ni<sub>35wt</sub> [8] as the best candidates.

We developed a method, based on thermal oxidation in air, causing an increase of  $R_{C,Mgn}$  of the Sn<sub>95wt</sub>Ag<sub>5wt</sub> coated cables to the requested specified values. We learned about the microscopic processes determining  $R_c$ . Finally we tested the Cu<sub>55wt</sub>Sn<sub>45wt</sub> and Sn<sub>65wt</sub>Ni<sub>35wt</sub> coated cables.

In this paper we report on the new results and we make reference to [7] when necessary. In Section II we explain modifications to the method for  $R_c$  measurement. Section III is a summary on chemical analysis of Sn<sub>95wt</sub>Ag<sub>5wt</sub> strands. Section IV deals with the formation and evolution of contacts in the Sn<sub>95wt</sub>Ag<sub>5wt</sub> coated cables, and Section V with  $R_c$  in those cables. In Section VI we discuss  $R_c$  of the Cu<sub>55wt</sub>Sn<sub>45wt</sub> and Sn<sub>65wt</sub>Ni<sub>35wt</sub> coated cables. Although  $R_c$  is controlled in both cables 1 and 2, most of the work was done on cables 1.

We reserve the term “heat treatment” (HT) for the oxidizing treatment of cable done in order to increase  $R_c$ , typically in 200 °C dry air; the term “curing” for the application of pressure and elevated temperature to the wound coil. As a part of the  $R_c$  test we simulate the effect of curing on the cable by heating the cable sample in the sample holder and under pressure to the same temperature and for the same duration as the coil in curing. We call this process curing as well.

## II. DC ELECTRICAL METHOD FOR MEASUREMENT OF $R_c$ ON CABLE SAMPLES

As the system and the method for the DC electrical measurement of  $R_A$  and  $R_c$  in cables were described in detail in [7], we outline the principle and the sequence of measurements.

We do not measure in magnetic field anymore, as the induced change in  $R_C$  is negligible for cables with SnAg coated and oxidized strands.

The measurements were done at 4.2 K, and at the pressure onto the cable of 50 MPa.

#### A. Principle of the $R_A$ , $R_C$ Measurement [7]

A pressure of 50 MPa is applied to the broad face of a sample of cable. The sample is cooled down to 4.2 K. Current of up to 100 A is injected into two opposite strands. One of them is chosen as potential reference. The DC voltage on the strands of the cable against the potential reference is measured, and the  $R_A$  and  $R_C$  are evaluated from this distribution.

#### B. Sample Holder [7]

All  $R_C$  measurements reported in this paper were done using stainless steel sample holders (see Fig. 1) with a length of 240 mm. Each holder consists of a cradle, a piston, insulating strips, and a set of 24 M8 bolts with INVAR washers.

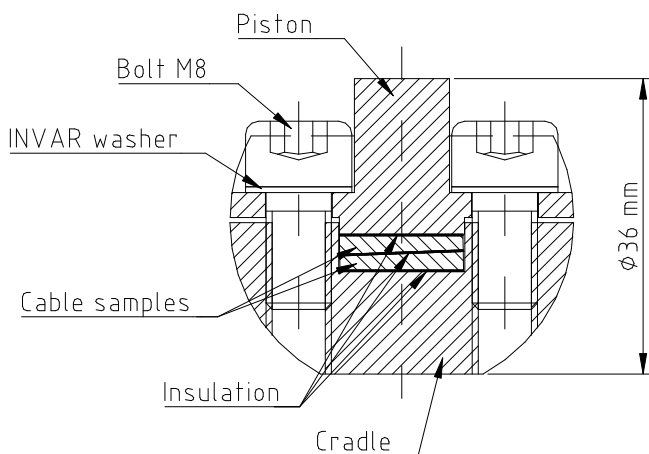


**Fig. 1.** The sample holder consists of the cradle, the piston, and the fastening bolts.

Two trapezoidal cable samples, insulated by a single wrap of 25  $\mu\text{m}$  thick polyimide foil, are inserted into the cradle in opposite directions, so that they have an overall rectangular cross-section. The piston is pushed against the cradle by the PTFE lubricated bolts, tightened at 7.5 Nm. The nominal pressure on the cables is 50 MPa.

#### C. The Sequence of Measurements

In order to obtain  $R_{C,Mnf}$ ,  $R_{C,Crd 160^\circ C}$ ,  $R_{C,Crd 190^\circ C}$ , and  $R_{C,Rlx}$ ,  $R_C$  is measured on each sample passing successively through the following stages: as manufactured/prepared ( $R_{C,Mnf}$ ), after curing at 50 MPa, 160  $^\circ\text{C}$  for 1h ( $R_{C,Crd 160^\circ C}$ ), after the standard curing at 50 MPa, 190  $^\circ\text{C}$  for 30 min ( $R_{C,Crd 190^\circ C}$ ), and after the pressure on the sample was relaxed overnight and restored ( $R_{C,Rlx}$ ).

The  $R_C$  tests are done on sets of 3 to 5 samples to obtain:

- $R_C$  of a particular cable.
- The uniformity of  $R_C$  along a HT cable.

- Which HT a cable needs in order to reach the required resistance after curing.

For c) we cut several samples of a cable and we heat treat them in 200  $^\circ\text{C}$  dry air for 4, 8, 12, and 16 h respectively. Then we trace the curves (see Fig. 2), showing how  $R_{C,Crd}$  depends on the duration of HT.

Each sample must be prepared with care and skill, since the flatness of the sample holder surfaces, the insulation of the sample and its position in the holder, and tightening of the

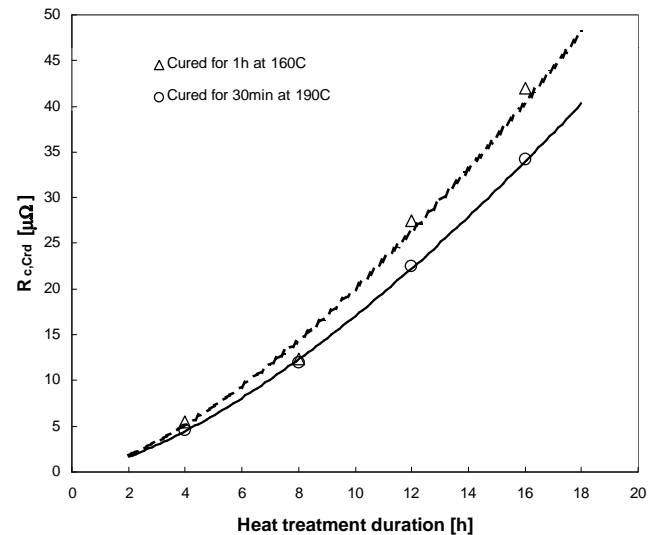


**Fig. 2.**  $R_{C,Crd}$  as a function of the heat treatment duration with the curing condition as parameter on  $\text{Sn}_{95\text{wt.}}\text{Ag}_{5\text{wt.}}$  coated cable.

bolts can affect the result. At least 3 cable samples have to be measured for a), 4 samples for c).

### III. ANALYSIS OF THE $\text{Sn}_{95\text{wt.}}\text{Ag}_{5\text{wt.}}$ COATED STRANDS

$R_C$  in the  $\text{Sn}_{95\text{wt.}}\text{Ag}_{5\text{wt.}}$  coated cables originates from a very thin layer of oxides on the strand surface. This section presents results of observations for the color of the strands, the chemical composition profile, and the “thickness” of the coating.

#### A. Appearance of Contact Surface

Will be described within Section IV.

#### B. Color of the Strands after HT

The  $\text{Sn}_{95\text{wt.}}\text{Ag}_{5\text{wt.}}$  coated strand is bright and shiny. After HT of the cable the strands become colored. The color pattern runs along the strand and changes only slightly in the contact areas.

We observed 3 types of color pattern: a) Rather uniform pattern. The main color is brass yellow, often covered with large ocher or blue to black stains or strips. The overall tone is clear. b) Fine linear structure. The lines are about 20  $\mu\text{m}$  wide, and their color is alternatively copper red, brass yellow, or dark blue to black. The overall tone is dark. c) Almost uniform gray to dark blue or black pattern, occasionally the brass yellow can be seen. The c) type corresponds to the dark areas seen on b).

The color pattern is characteristic for each cable manufacturer.

### C. Chemical Composition Profile

The chemical composition profile near to the strand surface was established by CSMA Ltd. [9] and by CERN by means of the Auger Electron Spectroscopy (AES). Over 70 AES profiles were measured on as-coated, HT, and cured strands, giving primary information about the metallurgical processes determining  $R_c$ .

*As-coated strands:* Next to the strand surface the composition profile is almost constant and close to  $Cu_3Sn$ . Starting at depth  $\delta_{1CuSn}$  the Cu concentration starts to increase at the expense of Sn, and reaches more than 95 at.% at depth  $\delta_{1Sn}$ . Typical values are:  $\delta_{1CuSn} = 0.2 \mu m$ ,  $\delta_{1Sn} \sim 0.4 \mu m$ .

*HT strands:* 2 types of composition profiles were measured:

- *Sn<sub>2</sub>O type of profile:* Near surface the O concentration follows that of Sn suggesting presence of Sn<sub>2</sub>O with only traces of Cu. After depth  $\delta_{2SnO}$  the Cu fraction rapidly increases and that of Sn decreases. Outside the oxide layer the composition is about  $Cu_{85at.\%}Sn$  at least as far as depth  $\delta_{2CuSn}$ . Typical values are:  $\delta_{2SnO} = 0.01 \mu m$ ,  $\delta_{2CuSn} \geq 0.5 \mu m$  (end of the AES profile). Strands have color pattern a).
- *Cu<sub>2</sub>O type of profile:* Near surface is a layer of Cu<sub>2</sub>O with thickness  $\delta_{2CuO}$  containing only traces of Sn. The thicker this layer, the darker is the color of the strand. From the end of the oxide layer the fraction of Sn first increases up to 10 at.%, and then remains level till depth  $\delta_{2Sn}$ . The rest is Cu. Typical values are:  $\delta_{2CuO} = 0.03$  to  $0.05 \mu m$ ,  $\delta_{2Sn} \geq 0.5 \mu m$  (end of the AES profile). All strands in the cable have color pattern b) or c).

*Cured strands:* 2 types of composition profiles were distinguished on the strands of the HT and cured cables:

- *Strands with Sn<sub>2</sub>O type profile after HT:* No obvious difference before and after the curing can be seen on the AES profile.
- *Strands with Cu<sub>2</sub>O profile after HT:* The profile is similar to the one after HT. The difference is in the Cu<sub>x</sub>O layer. While after HT, the composition was constant within the Cu<sub>x</sub>O layer, in cured cables the concentration of oxygen gradually decreases towards the interior of the strand.

### D. "Thickness" of the Coating

Some cables gain more  $R_c$  during HT than others. We also found that the  $R_c$ -drop due to the curing is related to the  $R_c$ -gain during HT: the greater the gain, the smaller the drop. We felt that thickness of the coating was a relevant parameter.

We have considered the following methods to measure the thickness of the coating: a) Metallurgical cut and observation under microscope, b) X-ray fluorescence, c) AES, d) Coulometry, and e) Chemical dissolution followed by Atomic Absorption Spectroscopy (AAS).

All cables produced during the last two years have coatings less than  $1 \mu m$  thick. Moreover, the coatings sensitive

to HT are about  $0.5 \mu m$  thick. Metallurgical cut followed by observation under microscope is too laborious for serial testing. The coating is too thin for optical microscope, and the result is a local characteristic. The X-ray fluorescence was not available when the work was performed. The AES is too expensive for serial testing. The result is even more local than the metallurgical cut. The coulometry would suite well but the coating thickness is at the limit of resolution of available instruments. Furthermore, the measurement would be disturbed by the complex metallurgical state of the coating layer. Finally we used chemical dissolution followed by AAS to measure the quantity of the coating.

*Description of the method:* 50 cm of strand is put into 25 ml of mixture of 6.2% H<sub>2</sub>SO<sub>4</sub> and 4.5 % H<sub>2</sub>O<sub>2</sub>, rest H<sub>2</sub>O at room temperature. The surface layer of the strand of about  $20 \mu m$  thick is dissolved. The concentration of Sn (Ag) in the solution is measured by the AAS. The amount of Sn (Ag) per unit of length of the strand is calculated. The analysis takes about 30 min/sample.

The result of this measurement is the quantity of Sn (Ag) near to the strand surface. Even though the Sn forms an alloy with Cu, and the thickness of the coating is hard to define, we can calculate the effective coating thickness. It is the thickness that the measured quantity of Sn<sub>95wt.</sub>Ag<sub>5wt.</sub> would have, had it just covered the strand without penetrating inside. The quantity of Ag is expressed as fraction of SnAg.

We keep in mind that the strand coating material does not form a separate and uniform layer in real cables as: a) The amount of the deposited coating material varies locally depending on the cross section of the bare strand and on the coating tools and procedure. b) During the coating and perhaps during the cabling the coating material diffuses into the Cu matrix of the strand and Cu diffuses into the coating. c) The unalloyed soft coating material is displaced, likely scraped off the most exposed part of the contact during the cabling. The quantity of coating becomes smaller within the contact area compared to the rest of the strand. What remain are mainly the hard  $Cu_3Sn$  intermetallic layer and the Cu matrix of the strand. d) The rest of the pure coating diffuses during HT.

*Measurement of effective thickness on HT cables:* We would like to use the described method to HT cables as well. We compared the effective thickness measured on samples of 8 different cables before and after HT. For 7 cables the method indicated  $-10 \pm 7 \%$  less Sn after HT. For one cable the difference was  $+21 \%$ . The origin of the difference may be a fraction of Sn in the HT cables, perhaps in the form of oxide that did not dissolve. Adjustment of the solvent might further improve the accuracy.

*Measurement of the concentration of Ag:* The fraction of Ag in the coating of cable may affect the sensitivity of  $R_c$  to HT. The fraction of Ag in SnAg was measured in 10 cables and was found  $2.4 \pm 0.2$  at.% in 7 cables, and  $1.22 \pm 0.03$  at.% in 3 cables.

### E. Comparing $R_c$ with the results of analysis

We can correlate  $R_c$  to the result of visual or chemical analysis. When doing so, we keep in mind that each measu-

red  $R_c$  represents a mean value over 1500 or 2900 contacts (Cable 1 or 2) between crossing strands.

*Comparing  $R_c$  with the color pattern.* Since both the color and the contact resistance depend largely on the surface oxidation, the color pattern is a useful guide in assessing  $R_c$  of the cable.

*Comparing  $R_c$  with the AES results.* The AES analysis is done on an area of about  $20 \times 30 \mu\text{m}$ . As one  $R_c$  measurement refers to an area of  $3.2 \times 10^6$  AES analyses, we do not directly correlate the composition profiles to the measured values of  $R_c$ . We only establish the typical chemical composition of different types of strands.

*Comparing  $R_c$  with the effective thickness and the Ag concentration:* The effective thickness is a macroscopic parameter based on the assumption that all the coating material uniformly covers the strand. Later we will correlate the effective thickness to  $R_c$ .

#### IV. EVOLUTION OF CONTACTS IN THE $\text{Sn}_{95\text{wt.}}\text{Ag}_{5\text{wt.}}$ COATED CABLES

When controlling  $R_c$  in the magnets, it is useful to understand how the contacts have evolved before.

In the  $\text{Sn}_{95\text{wt.}}\text{Ag}_{5\text{wt.}}$  coating process the strand passes first through a cleaning bath, then through a bath of molten  $\text{Sn}_{95\text{wt.}}\text{Ag}_{5\text{wt.}}$ . At that stage, part of the coating material forms an alloy with the strand Cu matrix. For thick coatings, the rest of  $\text{Sn}_{95\text{wt.}}\text{Ag}_{5\text{wt.}}$  remains on the surface.

During cabling the contacts between strands are formed by plastic deformation. The contacts between the crossing strands grow elliptical and those between adjacent strands grow flat. The deformation starts by scraping off the soft unalloyed rest of  $\text{Sn}_{95\text{wt.}}\text{Ag}_{5\text{wt.}}$ . The following layer, rich in  $\text{Cu}_3\text{Sn}$ , is hard, fragile, and adheres well to the Cu matrix. As the deformation continues this layer breaks together with the Cu matrix into several  $\mu\text{m}$  sized segments. The segments separate in the direction perpendicular to the strand axes [11] and pave the zone of the highest deformation. The surface of the opposite contact can show superposition rather than separation of segments [12].

The contact between crossing strands has the form of a stretched ellipse with a long to short axes ratio of about 3, and an average surface of  $1.25 \text{ mm}^2$  for Cable 1 [8]. Two regions can be distinguished by visual observation: the peripheral zone and the central zone.

The peripheral zone was formed last and reflects the early stage of the deformation. At 70 x enlargement the surface of the coating is smooth and continuous. At 1000 x enlargement the surface shows traces of spread and flow of  $\text{Sn}_{95\text{wt.}}\text{Ag}_{5\text{wt.}}$  [10, 11, 12].

The central zone fills an ellipse covering  $1/3$  to  $1/2$  of the whole contact in the direction of its long axis. Its axial part is deformed first and reflects the strongest deformation. At 70 x enlargement the surface looks rough, and Cu shines together with the  $\text{Sn}_{95\text{wt.}}\text{Ag}_{5\text{wt.}}$ . At 3000 x enlargement the pavement of several  $\mu\text{m}$  large segments described above can be seen [10, 11, 12].

The complex color pattern (III. b), which appears on the strand surface after HT, originates in a longitudinal fine structure of the strand surface. The pattern becomes somewhat fuzzy in the axial area of the contact but on the rest of the surface it is undamaged and only slightly displaced in the direction perpendicular to the strand axis.

During HT, two scenarios are possible:

- Residuum of pure coating on the strand surface oxidizes faster than it alloys with the Cu matrix. The  $\text{Sn}_2\text{O}$  layer protects the surface and prevents Cu from reaching it. The Cu appears only deeper in the strand without link to O.
- Sn alloys with the Cu matrix too fast to form the  $\text{Sn}_2\text{O}$  layer on the surface. Cu reaches the surface and oxidizes to  $\text{Cu}_2\text{O}$ . The concentration of Sn is very low within the oxidized Cu layer. It increases deeper into the strand.

Those cables that gain readily  $R_c$  during HT contain almost uniquely the  $\text{Cu}_2\text{O}$  covered strands. Therefore we believe that the  $\text{Cu}_2\text{O}$  oxide layer determines  $R_c$ .

During curing the cable is compressed and heated up to  $190^\circ\text{C}$  for 30 min. The access of O to the contact surface is restricted, and part of the O from the  $\text{Cu}_2\text{O}$  layer dissolves inside the strand.  $R_c$  of the cable decreases.

Non-coated strands would form resistive layers more readily and reach very rapidly very high  $R_c$ . However O would easily dissolve during curing, and  $R_c$  would drop strongly [7]. The  $\text{Sn}_{95\text{wt.}}\text{Ag}_{5\text{wt.}}$  forms a barrier rendering  $R_c$  stable and restricting it into a range suitable for the LHC magnets. It makes the oxidation process slow enough to be controlled on a spool of cable in oven.

#### V. $R_c$ IN CABLES WITH STRANDS COATED WITH $\text{Sn}_{95\text{wt.}}\text{Ag}_{5\text{wt.}}$

Since the publication of [7] we aimed to increase  $R_c$  of the  $\text{Sn}_{95\text{wt.}}\text{Ag}_{5\text{wt.}}$  coated strands, mainly by oxidation. After testing different methods, atmospheres and temperatures, we decided for HT in dry air at  $200^\circ\text{C}$ . In that atmosphere all considered cables 1 need between 4 and 20 h to form resistive layers on the strands that result in  $R_{c,\text{Crd}}$  of  $20 \mu\Omega$  after the standard curing.

In industry, specified lengths of cable will be wound on spools before passing a HT in air ventilated ovens. As the uniformity of the HT is prerequisite for the uniformity of  $R_c$ , care has to be taken that air can penetrate into the winding, that the thermal conductivity across the spool is not deteriorated by spacer or protective layers, and that the cable is not locally overheated. The HTs are long enough to preserve uniformity in duration and temperature of the treatment within the spool. The homogeneity of  $R_c$  of cable within one HT spool is now under evaluation.

The strand manufacturing process was optimized so that HT does not degrade the current carrying parameters of the cable. Moreover, it has positive secondary effects. Performed on finished cable, it removes the mechanical stress residing from cabling and improves the RRR of the copper matrix.

##### A. Sensitivity to HT

As mentioned in the previous section, the sensitivity to oxidation, and thus the required HT duration, depends on the

quantity of coating on the contact, and on its metallurgical status. As the quantity of Ag on the strand is fixed through the controlled concentration of Ag in the coating bath, and the metallurgical status is determined by the cable manufacturing procedures, the main free parameter is the amount of Sn.

Fig. 3 shows the main  $R_C$  related parameters as function of the effective coating thickness: a)  $R_{C,Mnf}$  of the HT cable for HT of 200 °C, 8 h, dry air. b)  $R_{C,Crd}$  of the HT and cured cable for HT as of a) and curing of 30 min at 190 °C. c) The  $R_C$ -drop equal to  $R_{C,Mnf}/R_{C,Crd}$ . While the curves a) to c) show  $R_C$  related parameters for the fixed HT duration of 8 h, the curve d) shows the HT duration in 200 °C dry air, needed to increase  $R_C$  so that the after the 30 min, 190 °C curing the cable reaches 20  $\mu\Omega$ .

In spite of the complex nature of a contact, the link between the sensitivity to HT and the effective coating thickness is obvious. The spread of points is mainly caused by differences in procedures among the strand and cable manufacturers.

The plot shows the following:

- The effective thickness of 0.5  $\mu\text{m}$  is needed to get  $R_C = 20 \mu\Omega$  after the HT during 8 h.
- The  $R_C$ -drop, which causes uncertainty in  $R_C$  in real magnets, decreases with decreasing coating thickness, and is 4.3 for 0.5  $\mu\text{m}$  effective thickness.
- There is considerable freedom in the choice of HT duration providing the corresponding effective thickness can be maintained.
- It is not necessary, in principle, to measure any of the curves shown in Fig. 2 to obtain the required HT duration for a cable. This time consuming operation can be substituted by the measurement of the effective thickness, and the HT duration can be found from Fig. 3.

### B. Sensitivity to Curing

The  $R_C$ -drop due to the curing depends on the curing temperature, pressure, and duration. Until now we have not measured the sensitivity to the curing pressure and duration.

We estimate the relative sensitivity to the curing temperature  $\frac{1}{R_{C,Crd}} \frac{dR_{C,Crd}}{dT_{Crd}}$  to  $-6$  to  $-8 \times 10^{-3} \text{ K}^{-1}$  for cables HT during 8 h. This means that the average  $R_C$  decreases by 1.5  $\mu\Omega$  in a coil cured at 200 instead of 190 °C. Our estimation is based on the difference in  $R_{C,Crd}$  of samples cured at 160 °C and at 190 °C. The estimation is optimistic, as the diffusion rate and thus the  $R_C$ -drop will be higher close to the 190 °C than over the whole interval of 160 to 190 °C.

## VI. $R_C$ IN CABLES WITH STRANDS COATED WITH $\text{Cu}_{55\text{wt.}}\text{Sn}_{45\text{wt.}}$ AND $\text{Sn}_{65\text{wt.}}\text{Ni}_{35\text{wt.}}$

In [8] two electrolytic coating materials were found promising with respect to their  $R_C$ : the  $\text{Cu}_{55\text{wt.}}\text{Sn}_{45\text{wt.}}$  and the  $\text{Sn}_{65\text{wt.}}\text{Ni}_{35\text{wt.}}$ . In order to measure all  $R_C$  relevant data, Cable 1 type strands were coated with a 1  $\mu\text{m}$  thick layer of each of these materials, and cables were manufactured.

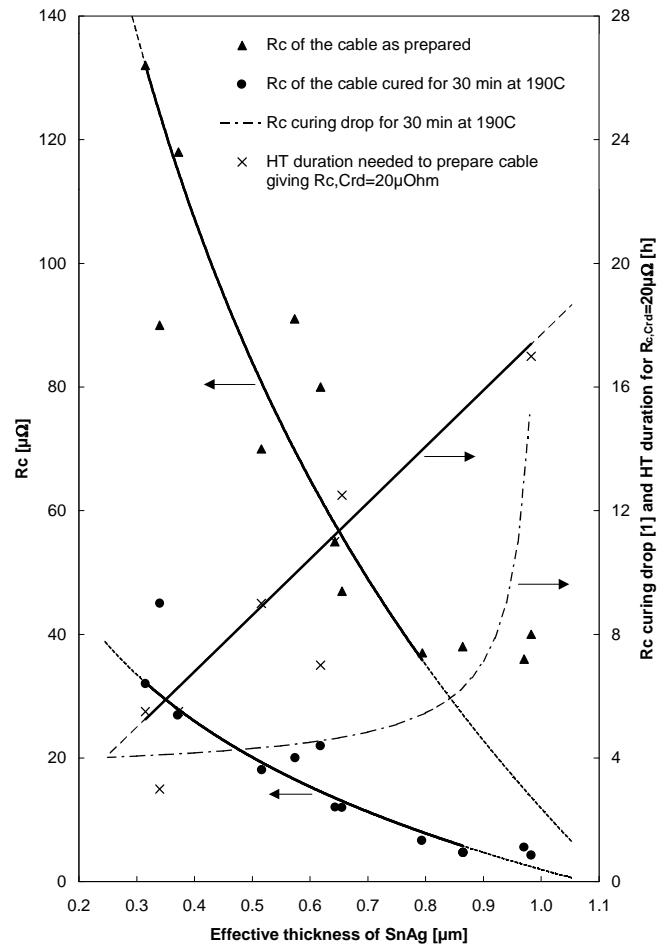


Fig. 3. Impact of the effective coating thickness on the main  $R_C$  characteristics.

### A. Cable with the $\text{Cu}_{55\text{wt.}}\text{Sn}_{45\text{wt.}}$ Coated Strands

As manufactured the cable had  $R_C$  of 90  $\mu\Omega$ , which dropped to a very low value of 2.2  $\mu\Omega$  after the standard curing. However HT in 200 °C dry air, as short as 5 min, raised  $R_C$  to 600  $\mu\Omega$  in the as prepared state, followed by 130  $\mu\Omega$ , after the standard curing.

### B. Cable with the $\text{Sn}_{65\text{wt.}}\text{Ni}_{35\text{wt.}}$ Coated Strands

As manufactured, the cable had  $R_C$  of 65  $\mu\Omega$  that dropped to 12  $\mu\Omega$  after the standard curing. As  $R_{C,Crd}$  is not much below 15  $\mu\Omega$ , the coating would still be interesting for the use in coils. Moreover, adding more Ni in the compound could increase  $R_C$ . The  $\text{Sn}_{65\text{wt.}}\text{Ni}_{35\text{wt.}}$  coating does not need any HT.

The advantages of the electrolytic coatings are the better control of the coating process, and the shortness or absence of the HT. The inconveniences are: a) Higher price. b) Being close to intermetallics, these coatings are much harder than the molten bath deposited  $\text{Sn}_{95\text{wt.}}\text{Ag}_{5\text{wt.}}$ . Strands coated with  $\text{Cu}_{55\text{wt.}}\text{Sn}_{45\text{wt.}}$  or  $\text{Sn}_{65\text{wt.}}\text{Ni}_{35\text{wt.}}$  cause problems during cabling.

Although the electrolytic coatings are not foreseen for the cables of the main LHC magnets, they remain candidates if higher contact resistances are needed for special magnets.

## VII. CONCLUSIONS

The  $\text{Sn}_{95\text{wt.}}\text{Ag}_{5\text{wt.}}$  coating was selected for the production of the LHC main magnets' cables. It is cheaper than the electrolytic coatings, it has been widely used in the superconductor industry, and it does not perturb the cabling process.

In order to obtain  $R_{\text{C,crd}}$  of  $20 \mu\Omega$ , the quantity of deposited material is kept low, and a special HT in  $200^\circ\text{C}$  air was added after cabling. As a secondary effect, this HT removes the residual mechanical stresses introduced during cabling, and improves the RRR of the strand Cu matrix.

The strand manufacturing was modified so that the additional HT does not deteriorate the current carrying capacity.

The AES analysis showed that Cu, diffusing through the coating to the surface, and oxidizing there during HT, is essential for the buildup of  $R_{\text{C}}$  in the  $\text{Sn}_{95\text{wt.}}\text{Ag}_{5\text{wt.}}$  coated strands. It seems that during the coil curing, the Sn embedded deep in the Cu matrix prevents the O, concentrated in the vicinity of the surface, from escaping in the depth of the Cu matrix. Sn reduces the  $R_{\text{C}}$ -drop during coil curing to an acceptable value in contrast to the cables with bare Cu strands.

The quantity of the deposited coating material has a major effect on the increase in  $R_{\text{C}}$  during HT. The effective thickness of  $0.5 \mu\text{m}$  is needed for HT to take the acceptable 8 h. During the mass cable production the relatively simple measurement of the effective thickness can be used as an industrial control process parameter in order to check the coating, and to tune the HT duration.

Two cables with electrolytic coating, the  $\text{Cu}_{55\text{wt.}}\text{Sn}_{45\text{wt.}}$  and the  $\text{Sn}_{65\text{wt.}}\text{Ni}_{35\text{wt.}}$ , were tested. Though they will not be used for the main LHC magnets, they, may prove suitable for magnets requiring larger  $R_{\text{C}}$ .

## ACKNOWLEDGMENT

The authors are very grateful to J-M. Depond, A. Ghosh (BNL), G. Spigo and A. P. Verweij for their advises and all the fruitful discussions. They would like to thank in particular R. Cordier and J. Stott who prepared and measured  $R_{\text{C}}$  on a great number of cable samples, Z. Charifoulline (IHEP) for the development of the measurement software, D. M. Latorre (CERN EST/SM) and the CSMA for the AES analysis, C. Knoblauch and G. Delporte (CERN EST/SM) for the AAS analysis, A. Arn for the design of the sample holder, and C-H. Denarié and P. F. Jacquot for their daily efficient support in the laboratory.

Special thanks to the companies fabricating the superconducting cables for the LHC: Alstom (F), Europa Metalli (I), Furukawa (J), NEEW (USA), Outokumpu (SF), and Vaccumschmelze (D), who carried out additional development work and modified their technology in order to control the coating process, and to incorporate the cable HT.

## REFERENCES

- [1] *The Large Hadron Collider - Conceptual Design*, CERN/AC/95-05, 1995.
- [2] M. N. Wilson, R. Wolf, "Calculation of minimum quench energies in Rutherford cables", *IEEE Trans. Appl. Supercond.*, Vol. 7, pp. 950-953, No. 2, 1997.
- [3] A. P. Verweij, *Electrodynamics of Superconducting Cables in Accelerator Magnets*. PhD thesis, Universiteit Twente Enschede, 1995.
- [4] A. P. Verweij, R. Wolf, "Field errors due to inter-strand coupling currents in the LHC dipole and quadrupole", CERN Internal Note AT/MA 94-97, 1995.
- [5] R. Wolf, CERN, personal communication, 1998.
- [6] A. P. Verweij, CERN, personal communication, 1996.
- [7] D. Richter, J. D. Adam, J-M. Depond, D. Leroy, L. R. Oberli, "DC Measurement of electrical contacts between strands in superconducting cables for the LHC main magnets", *IEEE Trans. Appl. Supercond.*, Vol. 7, pp. 786-792, No. 2, 1997.
- [8] J-M. Depond, D. Leroy, L. Oberli, D. Richter, "Examination of contacts between strands by electrical measurement and topographical analysis", *IEEE Trans. Appl. Supercond.*, Vol. 7, pp. 793-796, No. 2, 1997.
- [9] CSMA Limited, Armstrong House, Oxford Road, Manchester M1 7ED, United Kingdom, 1995-1997.
- [10] J. D. Adam, J. P. Bacher, R. Cosso, J. M. Dalin, D. Lacarrère, S. Sgobba, "Caractérisation du revêtement d'étain sur la gaine en cuivre des câbles supraconducteurs pour applications au LHC", CERN/MT-SM-MI/95-015/SS, 1995.
- [11] D. Clair, "Câbles supraconducteurs: Etude des dégradations d'origine tribologique", MSc thesis, Institut National des Sciences Appliquées de Lyon, INSA, Lyon, France, 1994.
- [12] S. Lucas, "Tribologie de câbles supraconducteurs. Cas du LHC.", MSc thesis, Institut National des Sciences Appliquées de Lyon, INSA, Lyon, France, 1996.